

## **POROELASTIC MODELLING OF CSF CIRCULATION VIA THE INCORPORATION OF EXPERIMENTALLY-DERIVED MICROSCALE WATER TRANSPORT PROPERTIES**

**John C. Vardakis<sup>1</sup>, Liwei Guo<sup>1</sup>, Dean Chou<sup>2</sup>, Brett J. Tully<sup>3</sup>, Gry F. Vindedal<sup>4</sup>, Vidar Jensen<sup>4</sup>, Anna E. Thoren<sup>4</sup>, Klas H. Pettersen<sup>4</sup>, Stig W. Omholt<sup>4</sup>, Ole P. Ottersen<sup>4</sup>, Erlend A. Nagelhus<sup>4</sup> and Yiannis Ventikos<sup>1</sup>**

<sup>1</sup>Department of Mechanical Engineering, University College London, UK, {[j.vardakis](mailto:j.vardakis@ucl.ac.uk), [y.ventikos](mailto:y.ventikos@ucl.ac.uk)}@ucl.ac.uk

<sup>2</sup>Institute of Biomedical Engineering & Department of Engineering Science, University of Oxford, UK

<sup>3</sup>First Light Fusion Ltd, Begbroke Science Park, Oxfordshire, UK

<sup>4</sup>Institute of Basic Medical Sciences, University of Oslo, Oslo, Norway

### **SUMMARY**

We outline how multicompartmental poroelasticity is applied to the study of dementia. We utilize a 3D version of our poroelastic code to investigate the effects within parenchymal tissue. This system is coupled with multiple pipelines within the VPH-DARE@IT project which account for patient/subject-specific boundary conditions in the arterial compartment, in addition to both an image segmentation-mesh and integrated cardiovascular system model pipeline respectively. This consolidated template allows for the extraction of boundary conditions to run CFD simulations for the ventricles. Finally, we outline some experimental results that will help inform the MPET system.

**Key words:** *Dementia, Poroelasticity, Cerebrospinal Fluid, Glymphatic system, CFD, FEM*

### **1 INTRODUCTION**

Mild cognitive impairment (MCI) is defined as a state between normal ageing and dementia. It is defined as objective cognitive impairment relative to the person's age, with concern about the cognitive symptoms, in a person with essentially normal functional activities who does not have dementia [1].

The function of the brain depends on the transport of a multitude of fluids, namely blood, cerebrospinal fluid (CSF), interstitial fluid (ISF) and intracellular fluid. The ability to model these intertwined fluid transport processes within brain tissue in an anatomically accurate and patient-specific manner is of ever-increasing significance, especially since integrative systems possess numerous interactions with the external world which, either directly or indirectly, affect brain function and homeostasis.

Aquaporins (AQPs) are defined as a set of integral membrane transport proteins with a primary function of facilitating water movement across cell membranes in response to osmotic gradients. In this work, AQP4 is targeted as it is the most predominant aquaporin in the brain. It is located on the external and internal glial limiting membranes, the basolateral membrane of ependymal cells and astrocytes. In the latter, AQP4 occupies three key locations, namely the perivascular astrocyte end feet, perisynaptic astrocyte processes and in processes that involve  $K^+$  clearance, such as nonmyelinated axons and the nodes of Ranvier. This tactical distribution suggests that AQP4 controls water fluxes into and out of the brain parenchyma. AQP4 has been deemed to possess the essential role of controlling the water balance in the brain [2].

In the brain, it is understood that waste products and metabolites are transported by convection (incorporating diffusion and advection). Diffusion is the dominant transport mechanism for smaller molecules and shorter distances. However, studies have shown that advection may be the dominant transport mechanism for larger molecules [3] such as amyloid- $\beta$  [4], both within the perivascular spaces and within the brain's interstitium.

In a series of work by Nedergaard and colleagues proposed a glymphatic hypothesis [4], i.e., a clearance system based on a hydrostatic pressure difference between the periarterial and perivenous compartments drives advective water flow directed from the periarterial space, through

the astrocytic endfoot layer, extracellularly through the brain parenchyma and through the perivenous endfoot layer where it returns into the perivenous space. Furthermore, they showed that cerebral arterial pulsation drives the paravascular fluid exchange between CSF and ISF, and they have also shown the CSF-ISF exchange to be facilitated by astrocytic AQP4 [4]. This system is referred to as the *glymphatic system*.

The first goal of this work is to firstly develop Multiple-network Poroelastic Theory (MPET) based models capable of representing the aforementioned fluid transport processes in the cerebral environment. For these models to accurately represent the transport mechanisms taking place, parameters such as diffusion constants and water permeabilities are crucial. Experiments were therefore performed to address these parameters and variables, and the results incorporated within the developed poroelastic model. There were two types of experiments that took place: (i) intracranial pressure (ICP) recordings in response to injections of artificial cerebral spinal fluid and (ii) microscale imaging of tracer convection (diffusion and advection). This paper will focus on the prior. Both wild-type mice and mice lacking aquaporin AQP4 water channels in the astrocytes were used.

The second goal of the work is to portray the novelty of being able to link a Computational Fluid Dynamics (CFD) focused study with a 3D multi-compartmental poroelasticity solver which in turn allows for novel observations of cerebral fluid flow in the cerebroventricular system and its interaction with the surrounding parenchyma (for instance, observing swelling and/or draining in the periventricular region). In this way, we can investigate current developments in the field of dementia, such as whether sleep drives metabolic clearance from the brain, which ties together the glymphatic system, subject/patient-specific cerebroventricular modelling, various solution fields borne out of the subject/patient-specific MPET solver (for parenchymal tissue) and the experimental results that aid in outlining a more accurate use of parameters for this type of modelling platform.

## 2 METHODOLOGY

### 2.1 Multiple-Network Poroelastic Theory (MPET)

Poroelasticity is known to have numerous applications in biomedical engineering as well as soil mechanics and reservoir engineering. MPET is used to develop a spatio-temporal model of tissue displacement and fluid regulation in varying scales within the cerebral environment. The field equations are discretized using the finite-element method, and in all three spatial dimensions.

Specifically, the field equations of the MPET system stem from the fully dynamic, classical Biot system [5]. For a single compartment, this consists of the Navier equation representing momentum balance, and the Duhamel equation for the mass balance representing the diffusive Darcy fluid flow:

$$\begin{aligned} \rho \ddot{\mathbf{u}} - (\lambda + \mu) \nabla (\nabla \cdot \mathbf{u}) - \mu \nabla^2 \mathbf{u} + \alpha \nabla p &= \mathbf{f} \\ \gamma \dot{p} + \alpha \nabla \cdot \dot{\mathbf{u}} - \nabla \cdot \boldsymbol{\kappa}^* (\nabla p - \rho_f \mathbf{g}) &= s \end{aligned} \quad (1a, b)$$

In equations 1a and 1b,  $\rho$  represents the density of a porous and permeable matrix,  $\rho_f$  represents the density of the fluid,  $\lambda$  and  $\mu$  are the Lamé parameters (dilation and shear moduli of elasticity),  $\alpha$  is the Biot-Willis constant,  $\boldsymbol{\kappa}^*$  is the symmetric permeability tensor divided by the fluid viscosity,  $\gamma$  is the constrained specific storage coefficient,  $\mathbf{g}$  is the gravity vector,  $s$  is a source/sink term and finally,  $\mathbf{u}$  and  $p$  are the solid matrix displacement (mean displacement of particles forming the solid matrix) and the scalar pore pressure, respectively. In its current form, the MPET model comprises of four separate fluid compartments, arterial blood, arteriole/capillary blood, venous blood and CSF/ISF [5]. The resulting system of equations and finite element discretization template are described for a 2D application in [5]. Boundary conditions are applied through the VPH-DARE@IT project consolidated poroelastic pipeline and the literature [5].

### 2.2 Intracranial Pressure: Experimental procedures

The experiments were conducted on male adult (12–26 weeks, weighing 21–35 g) constitutive Aqp4<sup>-/-</sup> (n = 6) [3] with C57BL/6J mice as controls (n = 6). The animals were allowed ad libitum access to food and drinking water. The mice were anesthetized with an intraperitoneal injection of a

Zoletil-Xylazine-Fentanyl cocktail. Body temperature was monitored and kept at 37 °C. Tracheostomy was performed and mice mechanically ventilated with room air at 100 breaths per minute (bpm), volume 0.25-0.35 ml/min. Blood gases, blood pressure and oxygen saturation were monitored with a thigh sensor for mice. Oxygen saturation was at all times above 90%. A 30 GA needle connected to tubing and a 50 µl Hamilton syringe was inserted into the cisterna magna and fixed with tissue adhesive. A small craniotomy was made in the skull and the ICP catheter connected to a pressure transducer inserted 2 mm under the dura towards bregma. When a stable pressure was measured, baseline values were recorded for 1 min, before artificial cerebrospinal fluid (aCSF) was infused at 2 µl/min for 5 min by a pump, as described by Iliff et al., 2012. All experiments were performed in a manner that complies with Norwegian laws, and all protocols were approved by the Animal Care and Use Committee of the Institute of Basic Medical Sciences, University of Oslo, Norway.

### 2.3 Infusion test

The conventional interpretation of an infusion test (outlined in §2.2) is when the CSF production rate is temporarily altered over a finite period of time in order for CSF pressure to rise to a new plateau value before declining back to the original level once infusion has been halted. This type of test provides clinically useful outputs, such as the resistance to CSF outflow and cerebral compliance, which are both used by the MPET model. These two important parameters are estimated via a compartmental model of the form [6]:

$$\left[ e(p(t) - ICP_0)^{-1} \right] \frac{dp(t)}{dt} + \frac{p(t) - ICP_b}{R_{CSF}} = Q_{inf} \quad (2)$$

In the above,  $p(t)$  is the CSF pressure (mmHg),  $ICP_b$  is the baseline CSF pressure (mmHg),  $R_{csf}$  is the resistance to outflow (mmHg ml<sup>-1</sup> min),  $Q_{inf}$  is the infusion rate (ml min<sup>-1</sup>),  $C(p)$  is the compliance of the mouse brain (ml mmHg<sup>-1</sup>),  $ICP_0$  is the reference pressure (mmHg) and  $e$  is the cerebral elasticity (ml<sup>-1</sup>).

For constant infusion (as in in §2.2), the solution to Equation 2 is utilized, and  $e$  is calculated using a nonlinear least squares method (Levenberg-Marquardt) in MATLAB.

### 2.4 CFD based cerebroventricular fluid complexity

Flow through the multidimensional ventricles (obtained via T1-weighted acquisition) is solved using the Multiphysics software CFD-ACE+ (ESI Group, Paris, France) which is based on the finite volume approach, along with central spatial differencing, algebraic multigrid scheme and the SIMPLEC pressure–velocity coupling. The coupling between the poroelastic solver and the flow solver is achieved through appropriate CFD-ACE+ user-defined subroutines. Mesh generation for the cerebroventricular volumes was achieved via the use of CFD-VisCART (ESI Group, Paris, France), which is an unstructured adaptive Cartesian grid generation system. Boundary conditions for the inlets and outlets are obtained via the 3D MPET solver.

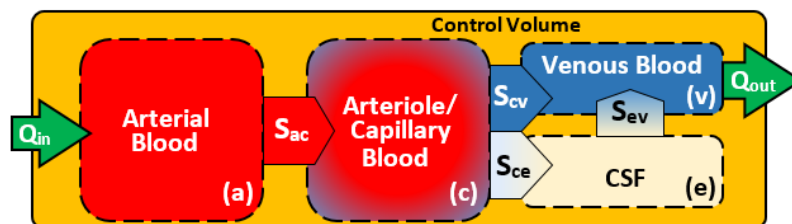


**Figure 1:** The fluid transfer restrictions placed between the four compartments (a) Flow is prohibited between the CSF/ISF and arterial network, whilst directional transfer exists between the  $a$  and  $c$ ,  $c$  and  $v$ ,  $c$  and  $e$  and  $e$  and  $v$  networks respectively [5].

### 3 RESULTS AND CONCLUSIONS

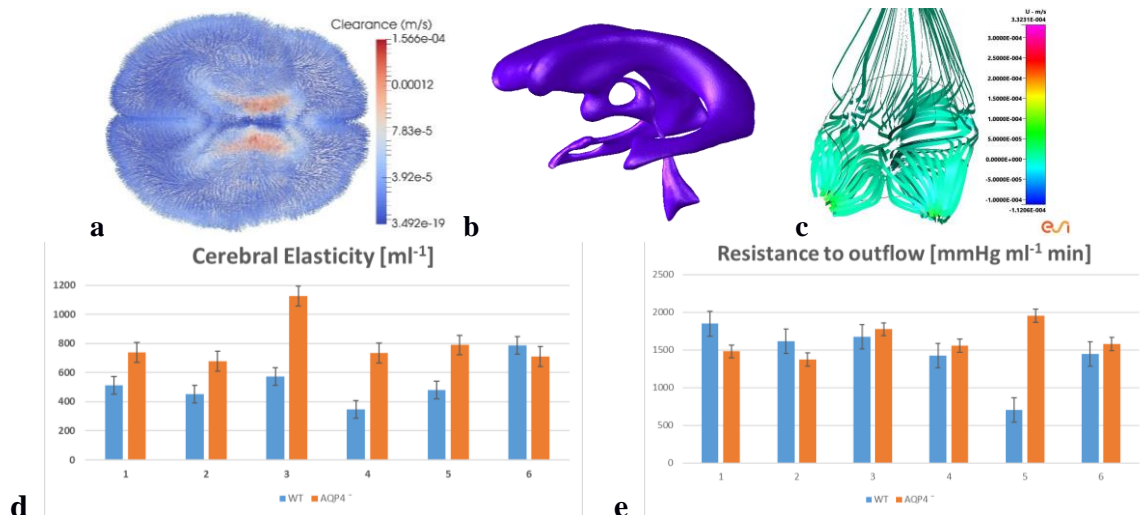


**Figure 2:** a) CSF/ISF clearance solution field within parenchymal tissue arising from the 3D MPET solver b) Ventricular geometry of a control subject used for the CFD simulations c) Streamlines merged with the  $u$ -component of velocity in the fourth ventricle of a control subject. d) Range of cerebral elasticity for AQP4-null and Wild Type (WT) controls. e) Range of resistance to CSF/ISF outflow for AQP4-null and WT controls. For the latter two plots, the visual arrangement of WT and AQP4-null data are paired according to the order of the respective set of experiments taking place.

In Fig. 2 above, we depict a selection of results from the broader context of this work. Utilizing the MPET solver pipeline within the VPH-DARE@IT project, we are able to use the research platform to acquire subject/patient-specific imaging data ( $\sim n = 50$  control and  $\sim n = 50$  MCI cases) to segment (see Fig. 2b) and mesh the parenchymal tissue volumes (linear tetrahedral elements) and cerebroventricular system. Permeability tensors that are generated from the principle eigenvector of the diffusion tensors are also included in the datasets. In the process, we also incorporate lifestyle data (such as ECG and blood pressure profiles over 24 hours) from the patients/subjects which create a subject profile that is supported by cardiovascular data. Both of these elements are feed an integrated open-loop cardiovascular model that provides the arterial compartment of the MPET system with the necessary boundary conditions in the cortical surface (applied to left/right cerebrum and cerebellum) and cerebral ventricles. One of the many solution fields of the MPET system is CSF/ISF clearance (see Fig. 2a). Others include parenchymal tissue displacement, CSF/ISF swelling, intracranial pressure, arterial and venous blood pressure and capillary perfusion.

Using the 3D MPET solver in this way allows us to extract CSF profiles at the inlet and outlet locations of the cerebroventricular system (lateral ventricles, foramen of Magendie, bilateral foramina of Luschka and central canal) over a window of time corresponding to an event of high or low activity (such as exercise and sleep), and thus running transient CFD simulations (see Fig. 2c) to assess the complexity of CSF flow within the ventricles for both control subjects and MCI patients. Preliminary results indicate abnormal peak aqueductal CSF velocities in a small group ( $n = 3$ ) of MCI patients (as high/low as  $\sim 11/0.8$  mm/s, compared to an average of around  $\sim 1-2$  mm/s) In this coupled setting, we are able to consider accounting for the influence of the glymphatic system within our work. The experimental results obtained in this study (see Fig. 2d, e) are currently being embedded within the MPET system, in order to give us a better theoretical understanding of the effects of AQP4 on the global response of the parenchymal tissue in the ageing brain (such as the link between mislocalization of AQP4 and amyloid-beta plaques [7]).

### REFERENCES

- [1] C. Cooper et al., Modifiable Predictors of Dementia in Mild Cognitive Impairment: A Systematic Review and Meta-Analysis. *American Journal of Psychiatry*, 172:4, 2015.
- [2] MC. Papadopoulos, AS. Verkman. Aquaporin water channels in the nervous system. *Nat Rev Neurosci*, 14:4, 2013.
- [3] AS. Thrane, et al. Filtering the muddied waters of brain edema. *Trends in Neurosciences*, 38:6, 2015.
- [4] JJ. Iliff et al. A Paravascular Pathway Facilitates CSF Flow Through the Brain Parenchyma and the Clearance of Interstitial Solutes, Including Amyloid. *Science Translational Medicine*, 4:147, 2012.
- [5] JC. Vardakis et al. Investigating cerebral oedema using poroelasticity. *Medical Engineering & Physics*, 38:1, 2016.
- [6] H. Juniewicz et al. Analysis of intracranial pressure during and after the infusion test in patients with communicating hydrocephalus. *Physiol Meas*, 26:6, 2005.
- [7] DM. Zeppenfeld et al. Association of Perivascular Localization of Aquaporin-4 With Cognition and Alzheimer Disease in Aging Brains. *JAMA Neurol*, 2016.